Osmotic ensemble methods for predicting adsorption-induced structural transitions in nanoporous materials using molecular simulations

Ji Zang, Sankar Nair, and David S. Sholl[a)]
School of Chemical & Biomolecular Engineering, Georgia Institute of Technology, 311 Ferst Drive NW, Atlanta, Georgia 30332-0100, USA

(Received 16 February 2011; accepted 12 April 2011; published online 9 May 2011)

Osmotic framework adsorbed solution theory is a useful molecular simulation method to predict the evolution of structural transitions upon adsorption of guest molecules in flexible nanoporous solids. One challenge with previous uses of this approach has been the estimation of free energy differences between the solid phases of interest in the absence of adsorbed molecules. Here we demonstrate that these free energy differences can be calculated without reference to experimental data via the vibrational density of states of each phase, a quantity that can be obtained from molecular dynamics simulations. We show the applicability of this method through case studies of the swelling behaviors of two representative systems in which swelling upon adsorption of water is of importance: single-walled aluminosilicate nanotube bundles and cesium montmorillonite. The resulting predictions show that the aluminosilicate nanotube bundles swell significantly with increasing interstitial adsorption and that the layer spacing of cesium montmorillonite expands up to about 12.5 Å, giving good agreement with experiments. The method is applicable to a wide range of flexible nanoporous materials, such as zeolites, metal-organic frameworks, and layered oxide materials, when candidate structures can be defined and a force field to describe the material is available. © *2011 American Institute of Physics*. [doi:10.1063/1.3586807]

I. INTRODUCTION

Structural transitions in nanoporous materials upon adsorption are important features of a variety of materials including metal-organic frameworks (MOFs) and zeolites.[1–4] These transitions can also be important in layered materials such as clays, where swelling due to the presence of solvents can occur. Although molecular simulation methods for predicting adsorption isotherms in rigid nanoporous materials are well known,[5] performing reliable simulations of materials that undergo structural transitions remains challenging. Progress towards this goal has been made in recent years with the introduction of osmotic framework adsorbed solution theory (OFAST),[6–9] an approach that can be used to predict the evolution of structural transitions upon adsorption in flexible nanoporous solids. When using OFAST, adsorption isotherms for a set of candidate rigid structures are calculated with standard methods, and OFAST defines a means of determining which adsorbate-filled structure has the lowest free energy at each state point of interest.

Key quantities needed to use OFAST are the relative free energies of the candidate solid phases in the absence of adsorbed molecules. In initial applications of OFAST to MOFs, this quantity was estimated by fitting predictions from simulations with observed structural phase transitions in experiments.[7,8] This approach has several difficulties: it can only be applied to materials for which experimental data are already available, and it is unclear how it could be applied to continuous transitions such as swelling. In this paper we demonstrate a method that avoids these difficulties. The main feature of this method is to directly calculate the free energy differences between different porous structures via analysis of the vibrational density of states (VDOS) calculated from harmonic vibrations of the framework.[10] The VDOS can be obtained from the Fourier transform of velocity correlation functions defined from standard molecular dynamics (MD) simulations.[11] We illustrate this method by studying the swelling of two guest-responsive materials, single-walled aluminosilicate nanotubes (NTs) and cesium montmorillonite, upon adsorption of water. These examples allow us to compare the predictions of our calculations with experimental results without fitting aspects of the structural transition to experiments.

II. METHODS

The osmotic ensemble is the appropriate thermodynamic ensemble to describe adsorption-induced structural phase transitions in a nanoporous material.[9] The osmotic potential during single-component adsorption is[7]

$$\Omega_{os}(T, P) = F_{host}(T) + PV - \int_0^P N_{ads}(T, p)V_m(T, p)dp, \quad (1)$$

where T, P, F_{host}, V, N_{ads}, and V_m are temperature, pressure, the free energy of the host phase in the absence of adsorbed molecules, the volume of the porous host, the number of adsorbed molecules inside the host, and the molar volume of the adsorbing species in its bulk state, respectively. If a host can exist in a variety of different structures, the structure that minimizes the osmotic potential will be the equilibrium state at the specified T and P. In using the osmotic potential in

a)Electronic mail: david.sholl@chbe.gatech.edu.

practical calculations, the preferred structure is the one that minimizes Ω_{os} with respect to the set of candidate structures that are examined. Once the host structure is defined (perhaps with appropriate constraints to maintain the structure), $N_{ads}(T,P)$ can be predicted with standard Grand Canonical Monte Carlo (GCMC) simulations.[12] Extensions of this idea have been developed to describe adsorption of gas mixtures.[8]

The main challenge with using Eq. (1) in a robust way is the calculation of F_{host}, the free energy of the porous structure when no adsorbed molecules are present. Assuming that a force field that allows MD simulations of the porous structure to be performed is available, this free energy can be calculated, within the quasiharmonic approximation,[10,13] by using data from a single MD simulation. This method has been used, for example, to calculate the free energy of several phases of elemental sulphur,[13] where it showed good efficiency and reliability compared with more demanding thermodynamic integration methods. First, the velocity autocorrelation function, $C(t)$, is calculated using data from an equilibrium MD simulation:

$$C(t) = \frac{\langle V(t) \cdot V(0) \rangle}{\langle V(0) \cdot V(0) \rangle}. \quad (2)$$

Here, V is velocity of an atom and $\langle\ \rangle$ denotes an average over all atoms in the system. The VDOS, $D(\nu)$, can be obtained via a Fourier cosine transform of $C(t)$:[11]

$$D(\nu) = \int C(t) \cos(\nu t) dt, \quad (3)$$

where ν is the vibrational frequency. By assuming the porous host is a harmonic crystal, the free energy can then be calculated[10,13] using

$$F_{host} = U_{conf} + \frac{1}{2} \int d\nu D(\nu) h\nu + k_B T \times \int d\nu D(\nu) \ln(1 - e^{-[h\nu/k_B T]}), \quad (4)$$

where U_{conf} is the average potential energy observed during the MD simulation. Below, we give examples of these calculations for two materials that undergo structure transitions during water adsorption, single-walled aluminosilicate NTs, and cesium montmorillonite.

III. RESULTS AND DISCUSSION

A. Swelling of single-walled aluminosilicate NTs

Single-walled aluminosilicate NTs have a highly ordered wall structure with isolated silanol groups bound on the inner surface of a nanotubular aluminum hydroxide wall,[14,15] as shown in Fig. 1. The presence of hydroxyl groups on this inner wall makes the interior of the pore hydrophilic and functionalizable by organic groups.[16] These properties make these materials attractive candidates for a variety of potential applications, including molecular separations, molecular encapsulation, and sensors. Synthesis of aluminosilicate NTs typically yields bundles of NTs rather than isolated NTs. In our previous work,[17] we have examined the adsorption of water in aluminosilicate NTs with flexible surface hydroxyl groups

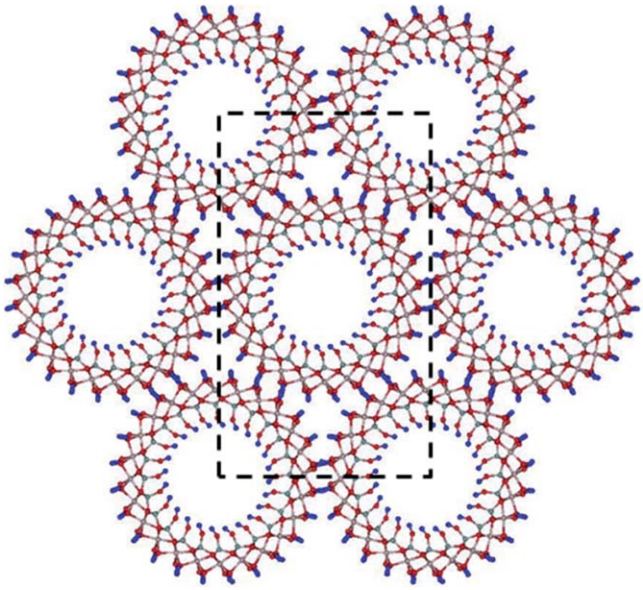

FIG. 1. Structure of hexagonally packed aluminosilicate NTs viewed along the axial direction with 24 Å spacing. Dotted lines indicate the simulation volume. Blue: hydrogen, red: oxygen, pink: aluminum, grey: silicon.

using GCMC simulations. These calculations showed that including the flexibility of these groups was critical to correctly model water adsorption in these NTs. This approach gave reasonable agreement with experimentally observed water isotherms at low and moderate water loadings. These experiments, however, suggest that at higher water loadings adsorption is strongly affected by swelling of NT bundles. Our previous simulations could not probe this behavior because they only allowed sorption in the pore of an isolated NT. Here, we use the OFAST method as described above to understand how important swelling of NT bundles is during water adsorption.

The details of construction and optimization of the NT structural models were described previously.[18–21] The nanotubes are taken to possess 24 Al atoms in the circumference, in agreement with the most of the published work on the structure of this material. Recent works suggest a possibility of larger numbers of Al atoms in the circumference,[22] but this is not taken into account in the present work since these suggestions are currently inconclusive. Periodic boundary conditions were used so that the NTs were hexagonally packed, similar to the experimentally observed monoclinic packing.[14] The unit cell employed in our simulations had an axial dimension of 2.52 nm (three times the axial repeat distance of the NT structure) and contained two NTs. To study the swelling of aluminosilicate NTs, we considered four candidate configurations with different NT-NT center to center spacings (24, 26, 28, and 30 Å), denoted below as NT24, NT26, NT28, and NT30. Note that this nomenclature does not refer to the number of Al atoms in the circumference, which is always taken as 24. The smallest spacing, 24 Å, is approximately the optimized spacing in the NPT ensemble for hexagonally packed NTs without water. For each spacing, we first found the most stable configuration by varying the relative position in the axial and circumferential directions for the two NTs in the unit cell

with the CLAYFF force field.[23] Then, NVT-MD simulations with a Berendsen thermostat were performed for 10 ps after equilibration of ~40 ps using the DLPOLY molecular simulation package[24] with a time step of 1 fs. In all of these calculations, the shape and volume of simulation cell were fixed. A small number of Al atoms were constrained to maintain the distance between two NTs and prevent them from clustering and buckling for NTs with non-equilibrium spacing. Velocities of non-fixed atoms were recorded to calculate the velocity autocorrelation function.

Adsorption isotherms were calculated at 298 K for water using the GCMC method as implemented in the MUSIC simulation code.[25] The CLAYFF force field[23] for NTs and the SPC model for water were used as in our earlier work. The flexibility of hydroxyl groups was considered as before,[17] with all atoms in the NTs being fixed in position except for the surface hydroxyl groups (this is different from our above MD simulations, in which most non-hydroxyl atoms in the NTs were not fixed). Other details can be found in the same work. The fugacity coefficients of SPC water at 298 K are close to unity at pressures up to 4 kPa.[26] We report our results by treating all vapors as ideal gases with the fugacity equal to the pressure.

Adsorption isotherms for water as computed using GCMC in NT bundles for the four candidate structures are shown in Fig. 2. At lower pressures, water molecules readily adsorb into the interstices when the NT-NT distances are small (NT24 and NT26). Significant amounts of water only adsorb in the interstices when the pressure is larger than ~0.03 (~0.1) kPa for NT28 (NT30). The adsorption of water inside the NTs is essentially the same in each configuration we considered in terms of both adsorption amount and threshold pressure (~0.1 kPa); all of the differences between the adsorption isotherms are associated with interstitial adsorption. Although larger loadings are observed for NTs with larger spacing, the adsorption isotherm for each configuration saturates at ~0.3 kPa. This is different from experimental[27,28] adsorption isotherms, which keep increasing until the saturation vapor pressure of water is reached. It seems likely that this occurs because of additional swelling of the NTs, although we cannot directly confirm this from our calculated data.

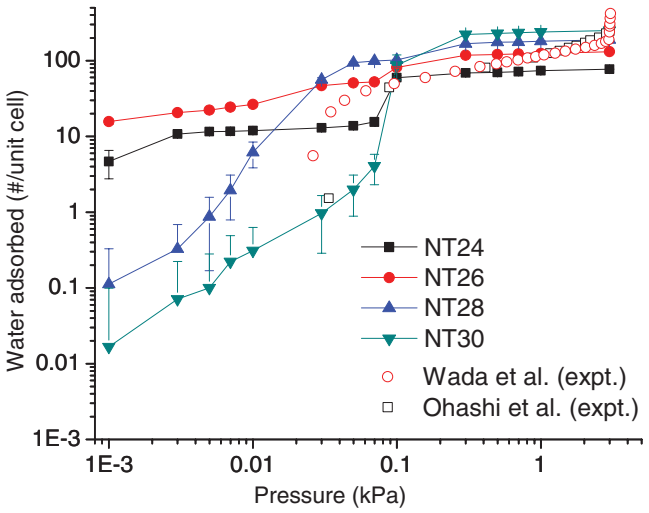

FIG. 2. Calculated adsorption isotherms of water in hexagonally packed aluminosilicate NTs, compared with experimental results from Wada and Yoshinaga (Ref. 27) and Ohashi *et al*. (Ref. 28).

TABLE I. Relative configurational energy and relative free energy for NT24, NT26, NT28, and NT30 in kcal/mol.

	NT24	NT26	NT28	NT30
U_{conf} -U_{conf}(NT24)	0	134.9	200.4	233.2
F-*F*(NT24)	0	33.6	52.8	69.1

We performed MD simulations to obtain the averaged configurational energy, U_{conf}, of each NT configuration with no adsorbed water and calculated the velocity autocorrelation function, $C(t)$, using Eq. (2). Sample velocity autocorrelation functions and vibrational density of states for NT24 and NT30 are shown in Fig. 3. Although the overall qualitative features of the VDOS are similar for the two structures, there are distinct differences between the two materials that lead to non-negligible differences in free energy. Table I shows the relative configurational energy and free energy for NT24, NT26, NT28, and NT30. If the configurational energy alone was used to estimate the free energy difference between the phases, the results would be quite inaccurate. The relative free energy increases as the NT spacing increases, consistent with the observation above that the 24 Å spacing minimizes the energy of the system when no water is present.

We then used Eq. (1) to calculate the relative osmotic potentials of the four phases as a function of water pressure, as shown in Fig. 4(a). At low pressures the first term on the right of Eq. (1) dominates and thus NT24 is most stable. With increasing pressure, the term defined by integration of the adsorbed amount becomes more important in comparing the osmotic potentials of different phases. At ~0.02 kPa, the osmotic potentials of NT26 and NT24 cross, and NT26 is favored at higher pressures. At still higher pressures, NT28 and then NT30 become favored. Our calculations indicate that bundles of aluminosilicate NTs swell significantly upon water adsorption. This material is a compelling example of why the free energy difference between phases cannot be simply approximated using U_{conf}; calculations with this approximation show no swelling in the pressures examined above.

The overall isotherm predicted by our calculations is shown in Fig. 4(b). This isotherm shows better agreement with experiment than the isotherms associated with any configuration with a fixed unit cell. In particular, the predicted overall isotherm is a continuous and smooth curve, an important feature that is not predicted by isotherms computed with a fixed unit cell. None of the computed isotherms are in good agreement with the available experimental data at the lowest pressures shown in Fig. 4(b). Possible reasons for this disagreement may include limitations of the experimental equipment at very low water vapor pressures, or a need for fine-tuning the force field to accurately predict the water-nanotube interactions at low pressures. The accuracy of the method in predicting a continuous swelling transition is dependent on the number of discrete configurations chosen for examination. The overall agreement between our calculations

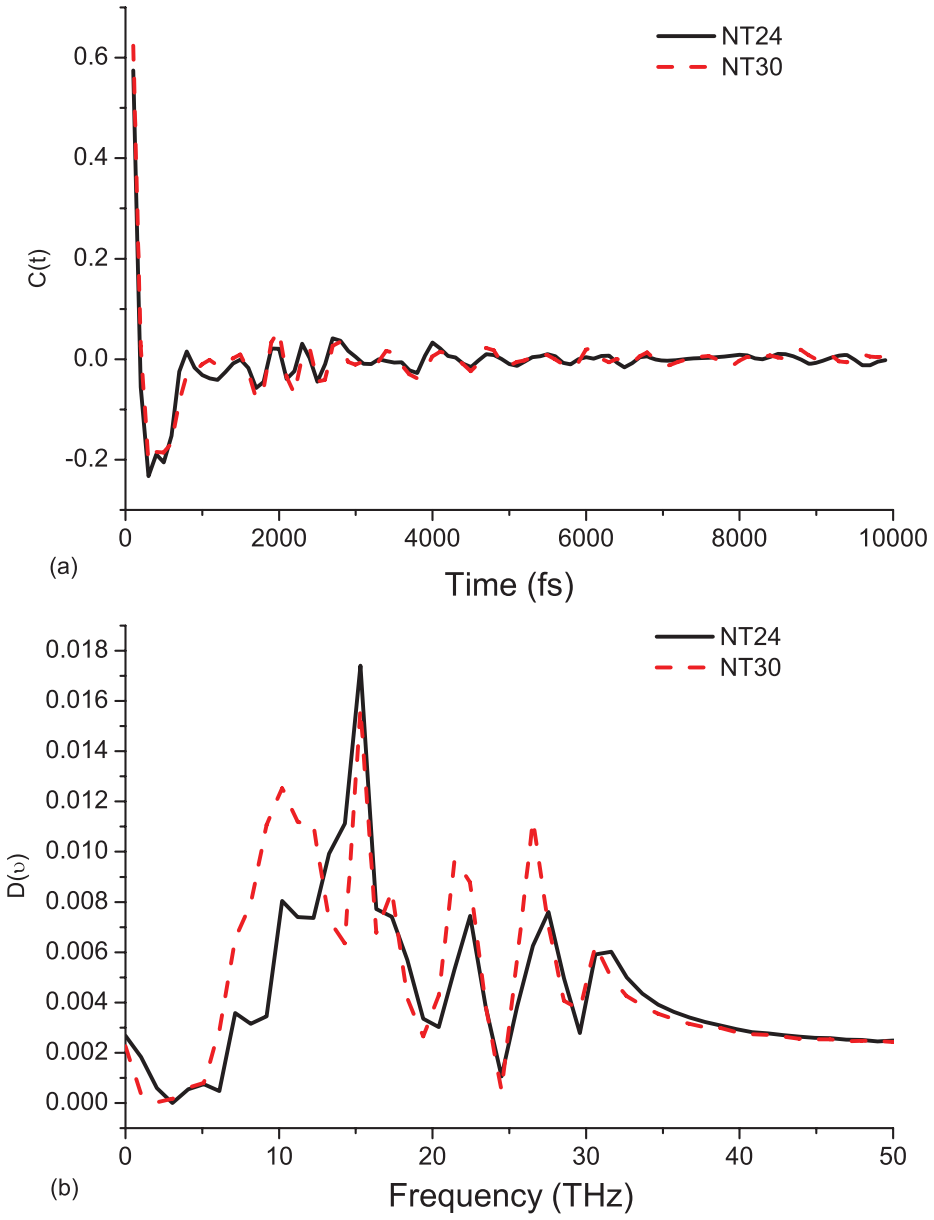

FIG. 3. (a) Velocity autocorrelation function and (b) vibrational density of states for NT24 and NT30.

and the experimental data, however, suggests that the swelling of AlSi NTs due to water adsorption is a continuous process. Our calculations also neglect the deformation of individual NTs, or changes in the NT packing angle. We performed a limited number of test calculations for well spaced NTs that suggested these deformation effects are minimal.

B. Swelling of cesium montmorillonite

As a second example of our method, we examine the swelling of montmorillonite. Montmorillonite is a dioctahedral smectite clay having monoclinic symmetry with two tetrahedral sheets (in which aluminum substitutes some of the silicon atoms) sandwiching a central octahedral sheet (in which magnesium substitutes some of the aluminum atoms).[29] The negatively charged aluminosilicate layers are balanced by metal cations such as Na^+, K^+, and Cs^+ located in the interlayer regions. One characteristic of these layered materials is their ability to adsorb water between the layers, resulting in large interlayer spacing expansions (as much as several times the original spacing). The swelling behavior of montmorillonite has been studied both by experiments[30–32] and simulations.[23,33–35] Combinations of MD and Monte Carlo simulations have been reported to mimic the experimental determination of the water adsorption isotherm.[33] A disadvantage of this previous simulation approach is that it can be difficult to achieve convergence during transitions that are associated with substantial free energy barriers.

To apply OFAST, a supercell composed of $4 \times 2 \times 2$ unit cells with composition $Cs_{12}(Si_{124}Al_4)(Al_{56}Mg_8)O_{320}(OH)_{64}$ was used to model cesium montmorillonite. As in the previous case, the CLAYFF force field[23] and the SPC model were used for clay and water. For montmorillonite with different layer spacing, optimization was performed first by considering

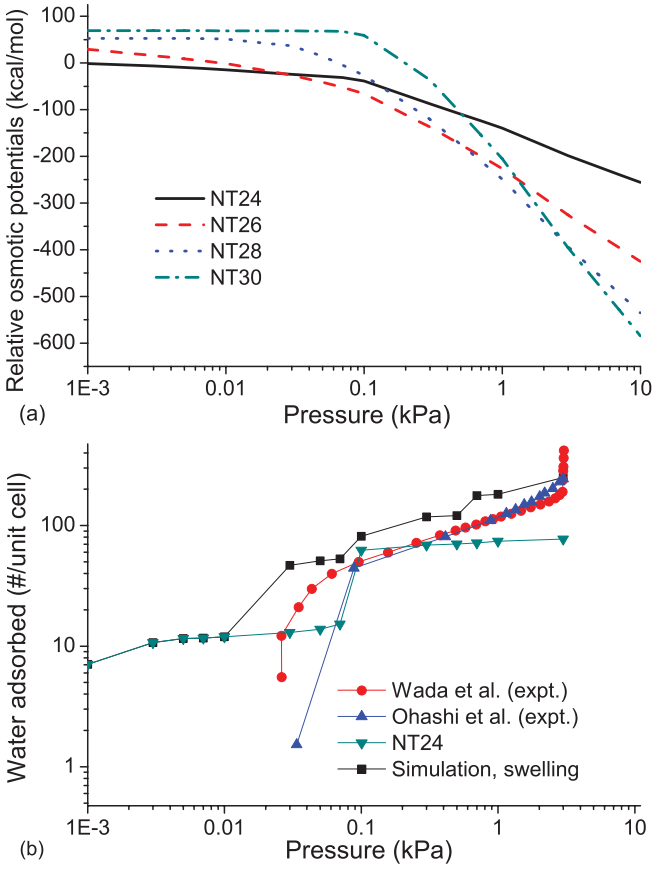

FIG. 4. (a) Relative osmotic potentials of NT24, NT26, NT28, and NT30 and (b) new adsorption isotherm obtained from thermodynamics analysis compared with experiments (Refs. 27 and 28) and that of NT24.

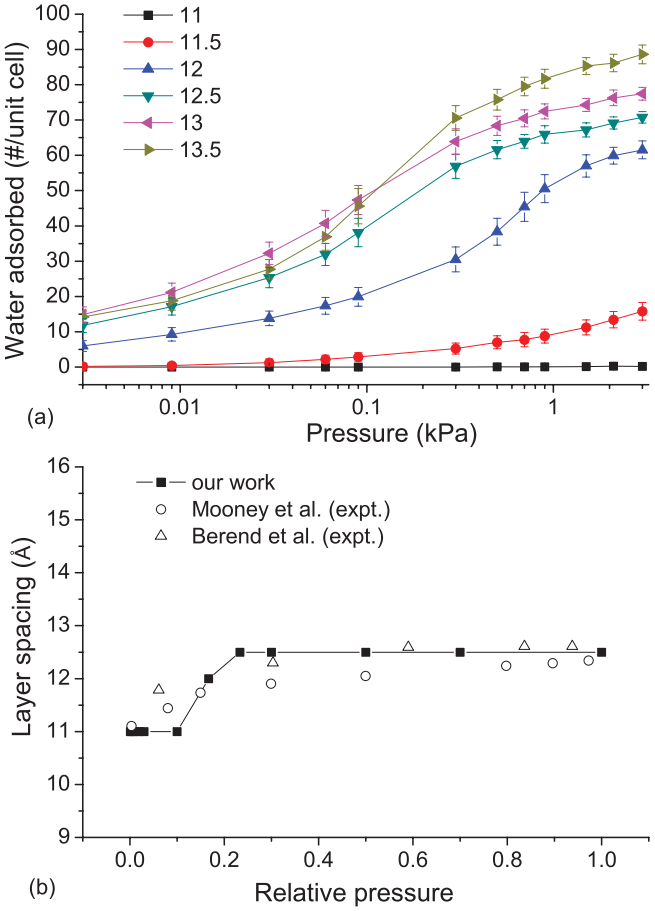

FIG. 5. (a) Water adsorption isotherms and (b) swelling curves from experiments (Refs. 30 and 32) and our prediction.

the relative position for the two parallel layers in the unit cell.[35] In the optimization and later MD simulations for the VDOS, a small number of Al atoms in the central octahedral sheet were fixed to maintain the distance between two layers. For each configuration examined, water adsorption was computed with GCMC in simulations that allowed the hydroxyl groups on the solid to be flexible. The positions of Cs atoms were unconstrained during these simulations, and these degrees of freedom were sampled with translational moves (but not insertions or deletions) during GCMC. Other simulation details were same as for the aluminosilicate NT calculations described above.

Figure 5(a) shows the calculated adsorption of water in cesium montmorillonite with layer spacings varying from 11 to 13.5 Å. There is no water adsorbed in the smallest spacing (11 Å) and for 11.5 Å the adsorption is much smaller than those in larger spacing clays. The relative osmotic potentials were obtained the same way as above. Among the layer spacings we considered, only spacings of 11 Å, 12 Å, and 12.5 Å are found to be physically observable. Clays with spacings of 11.5, 13, and 13.5 Å are not favored at any pressure because the amounts of adsorbed water in them are not large enough to compensate their higher free energies. This agrees with the swelling mechanism for montmorillonite that has previously been described as occurring in a discrete fashion.[30,33,35] The experimental swelling curves[30,32] displayed in Fig. 5(b) as open dots both show a layer-spacing plateau of ~12.5 Å, which is reproduced by our simulations. Our simulations only considered water adsorption in uniformly spaced interlayers. Experimentally, water can also adsorb on external surfaces and in interparticular mesopores.[36] Considering that the layer spacing determined from experiments is an average of a randomly interstratified (mixed-layer) structure,[37] our prediction is in good agreement with experimental results.

It is important to note that even for the largest layer spacing we studied, the configurations of cesium montmorillonite with and without the presence of water are very similar in terms of the distance of cesium to the clay surface. That is, the cesium ions are bound to the clay surface under all conditions we examined. A different situation occurs for sodium montmorillonite, whose layer spacing can increase to 18 Å or even larger upon adsorption of water[33] accompanied with the detachment of sodium ions from the clay surface. Our approach for computing the free energy of the adsorbent-free material and using it within OFAST becomes problematic in situations like this one.

IV. SUMMARY

In conclusion, we have studied the guest-responsive behaviors of single-walled aluminosilicate NTs and cesium montmorillonite upon adsorption of water via molecular simulations. Calculating the free energy of flexible phases via

their VDOS obtained from standard MD simulations enables us to predict their swelling using OFAST. This is a useful advance beyond earlier applications of OFAST, which relied on experimental data to estimate free energy differences of the adsorbing material. Our predictions agree well with experimental results for both cases: the aluminosilicate NTs undergo significant swelling and cesium montmorillonite does not show further swelling after reaching a layer spacing of about 12.5 Å. The method we have introduced will be useful for a wide range of flexible nanoporous materials such as MOFs when candidate structures can be defined and a force field to describe the adsorbing material is available. These conditions are fulfilled for many, although not all, materials of interest.

ACKNOWLEDGMENTS

This work was partially supported by NSF-CBET under Award Nos. 0966582, 0846586 (CAREER), and 0709090.

[1]C. Serre, S. Bourrelly, A. Vimont, N. A. Ramsahye, G. Maurin, P. L. Llewellyn, M. Daturi, Y. Filinchuk, O. Leynaud, P. Barnes, and G. Ferey, Adv. Mater. **19**, 2246 (2007).
[2]N. A. Ramsahye, G. Maurin, S. Bourrelly, P. L. Llewellyn, T. Devic, C. Serre, T. Loiseau, and G. Ferey, Adsorption **13**, 461 (2007).
[3]R. Kitaura, K. Fujimoto, S. Noro, M. Kondo, and S. Kitagawa, Angew. Chem., Int. Ed. **41**, 133 (2002).
[4]N. Floquet, J. P. Coulomb, G. Weber, O. Bertrand, and J. P. Bellatt, J. Phys. Chem. B **107**, 685 (2003).
[5]A. H. Fuchs and A. K. Cheetham, J. Phys. Chem. B **105**, 7375 (2001); R. Q. Snurr, A. T. Bell, and D. N. Theodorou, J. Phys. Chem. **97**, 13742 (1993).
[6]A. Boutin, M. A. Springuel-Huet, A. Nossov, A. Gedeon, T. Loiseau, C. Volkringer, G. Ferey, F. X. Coudert, and A. H. Fuchs, Angew. Chem., Int. Ed. **48**, 8314 (2009); F. X. Coudert, Phys. Chem. Chem. Phys. **12**, 10904 (2010); F. X. Coudert, C. Mellot-Draznieks, A. H. Fuchs, and A. Boutin, J. Am. Chem. Soc. **131**, 3442 (2009); F.-X. Coudert, A. Boutin, M. Jeffroy, C. Mellot-Draznieks, and A. H. Fuchs, Chem. Phys. Chem. **12**, 247 (2011); A. V. Neimark, F. o.-X. Coudert, C. Triguero, A. Boutin, A. H. Fuchs, I. Beurroies, and R. Denoyel, Langmuir **27**, 4734 (2011); A. V. Neimark, F. X. Coudert, A. Boutin, and A. H. Fuchs, J. Phys. Chem. Lett. **1**, 445 (2010); A. Boutin, F. o.-X. Coudert, M.-A. Springuel-Huet, A. V. Neimark, G. r. Feérey, and A. H. Fuchs, J. Phys. Chem. C **114**, 22237 (2010).
[7]F. X. Coudert, M. Jeffroy, A. H. Fuchs, A. Boutin, and C. Mellot-Draznieks, J. Am. Chem. Soc. **130**, 14294 (2008).
[8]F. X. Coudert, C. Mellot-Draznieks, A. H. Fuchs, and A. Boutin, J. Am. Chem. Soc. **131**, 11329 (2009).
[9]M. Jeffroy, A. H. Fuchs, and A. Boutin, Chem. Commun. (Cambridge) 3275 (2008).
[10]M. Born and K. u. Huang, *Dynamical Theory of Crystal Lattices* (Oxford University Press, New York, 1988).
[11]J. M. Dickey and A. Paskin, Phys. Rev. **188**, 1407 (1969).
[12]D. Frenkel and B. Smit, *Understanding Molecular Simulation: From Algorithms to Applications*, 2nd ed. (Academic, San Diego, 2002); M. P. Allen and D. J. Tildesley, *Computer Simulation of Liquids* (Oxford University Press, New York, 1987).
[13]C. Pastorino and Z. Gamba, J. Chem. Phys. **119**, 2147 (2003).
[14]S. Mukherjee, V. A. Bartlow, and S. Nair, Chem. Mater. **17**, 4900 (2005).
[15]P. D. Cradwick, K. Wada, J. D. Russell, N. Yoshinaga, C. R. Masson, and V. C. Farmer, Nature. Phys. Sci. **240**, 187 (1972); V. C. Farmer, M. J. Adams, A. R. Fraser, and F. Palmieri, Clay Miner. **18**, 459 (1983).
[16]D. -Y. Kang, J. Zang, C. W. Jones, and S. Nair, J. Phys. Chem. C **115**, 7676 (2011).
[17]J. Zang, S. Chempath, S. Konduri, S. Nair, and D. S. Sholl, J. Phys. Chem. Lett. **1**, 1235 (2010).
[18]S. Konduri, H. M. Tong, S. Chempath, and S. Nair, J. Phys. Chem. C **112**, 15367 (2008).
[19]S. Konduri, S. Mukherjee, and S. Nair, Phys. Rev. B **74**, 033401 (2006).
[20]S. Konduri, S. Mukherjee, and S. Nair, ACS Nano **1**, 393 (2007).
[21]J. Zang, S. Konduri, S. Nair, and D. S. Sholl, ACS Nano **3**, 1548 (2009).
[22]K. Tamura and K. Kawamura, J. Phys. Chem. B **106**, 271 (2002).
[23]R. T. Cygan, J. J. Liang, and A. G. Kalinichev, J. Phys. Chem. B **108**, 1255 (2004).
[24]See http://www.cse.scitech.ac.uk/ccg/software/DL_POLY/. DL_POLY is a package of molecular simulation routines: Smith, W.; Forester, T. R. DL_POLY; The Council for the Central Laboratory of the Research Councils: Daresbury Laboratory, Daresbury, Warrington, U.K., 1996.
[25]A. Gupta, S. Chempath, M. J. Sanborn, L. A. Clark, and R. Q. Snurr, Mol. Simul. **29**, 29 (2003).
[26]S. J. Wierzchowski and D. A. Kofke, J. Phys. Chem. B **107**, 12808 (2003).
[27]K. Wada and N. Yoshinaga, Am. Mineral. **54**, 50 (1969).
[28]F. Ohashi, S. Tomura, K. Akaku, S. Hayashi, and S. I. Wada, J. Mater. Sci. **39**, 1799 (2004).
[29]N. Guven, Rev. Mineral. **19**, 497 (1988).
[30]R. W. Mooney, A. G. Keenan, and L. A. Wood, J. Am. Chem. Soc. **74**, 1371 (1952).
[31]J. M. Cases, I. Berend, G. Besson, M. Francois, J. P. Uriot, F. Thomas, and J. E. Poirier, Langmuir **8**, 2730 (1992); W. J. Likos, Geotech. Test. J. **27**, 540 (2004).
[32]I. Berend, J. M. Cases, M. Francois, J. P. Uriot, L. Michot, A. Masion, and F. Thomas, Clays Clay Miner. **43**, 324 (1995).
[33]E. J. M. Hensen and B. Smit, J. Phys. Chem. B **106**, 12664 (2002).
[34]S. Karaborni, B. Smit, W. Heidug, J. Urai, and E. van Oort, Science **271**, 1102 (1996).
[35]D. A. Young and D. E. Smith, J. Phys. Chem. B **104**, 9163 (2000).
[36]F. Salles, J. M. Douillard, R. Denoyel, O. Bildstein, M. Jullien, I. Beurroies, and H. Van Damme, J. Colloid Interface Sci. **333**, 510 (2009).
[37]G. W. Brindley and G. Brown, *Crystal Structures of Clay Minerals and Their X-ray Identification*, New ed. (Mineralogical Society, London, 1980); M. F. Brigatti, E. Galan, and B. K. G. Theng, in *Developments in Clay Science*, edited by B. K. G. T. Faïza Bergaya and L. Gerhard (Elsevier, New York, 2006), Vol. 1, p. 19.